図 3 は難聴者との出会いの経験の有無と「可哀想」のイメージの有無の関係を示したものである。全体的に「可哀想」というイメージを持つ者は少なかったが、難聴者との出会いのない者は難聴者に対して「可哀想」というイメージを持つ者が 14.4% で、ある者のそれ (4.7%) より多かった。

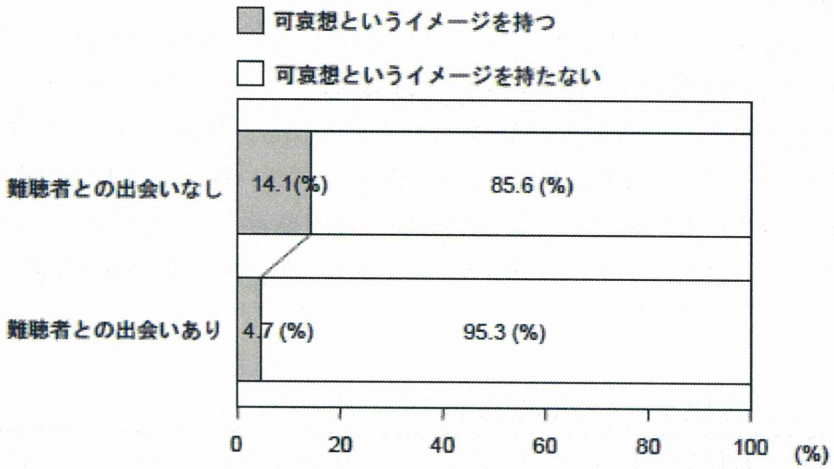

図 3. 難聴者との出会いの経験と「可哀想」というイメージの関係

図 4 は難聴者との出会いの経験の有無と難聴者に対しての「手話を使う」イメージの有無の関係を示したものである。難聴者との出会いのない者は難聴者に対して「手話を使う」というイメージを持つ者が 69.7% で、ある者のそれ (51.4%) より多かった。

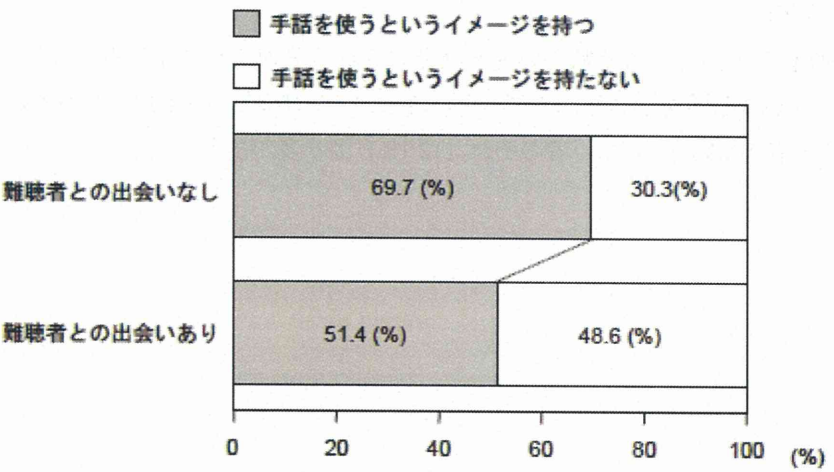

図 4. 難聴者との出会いの経験と「手話を使う」というイメージの関係

(6) 聴覚障害の聞こえ方の症状に対する認識

健聴者の難聴の症状に対する認識を把握するために、「聴覚障害を持つ人は音がどのように聞こえていると思いますか。」という質問を行った。なお、回答は複数回答可とした。回答は以下の表 2 の通りである。

「音が小さく聞こえる」と回答した者が 65.3% と一番多く、「ぼやけて聞こえる」と回答した者は 59.8% と過半数に達した。この 2 つの症状は認知度が高いと考えられる。これに対し、「とぎれて聞こえる」「雑音が入って聞こえる」の 2 つの症状はともに 20% 前後となった。「とぎれて聞こえる」症状とは、周波数によって聞き取りにくい音があり、その音が会話等の中に点在することで、全体の音の羅列の中でとぎれて聞こえるというものである。「雑音が入って聞こえる」症状とは、補聴器等を装用していると、聞き取りたい音 (会話等) と同様に雑音 (空調の音、机や椅子を動かす音等) まで拾い、音圧を増幅してしまうため結果として健聴者よりも雑音が大きく聞こえてしまうというものである。この 2 つの項目は他の 2 つの項目よりも認知度が低い傾向にあった。

表 2. 健聴者がもつ難聴者に対するイメージ

難聴の症状に対するイメージ	人数 (人)	パーセント (%)
音が小さく聞こえる	156	65.3
ぼやけて聞こえる	143	59.8
雑音が入って聞こえる	50	20.9
とぎれて聞こえる	43	18.0

n = 239 (複数回答可)

この質問において、難聴者との出会いの経験のある者と無い者の間で難聴の症状に対するイメージに有意に関連性があった項目は認知度の低い「とぎれて聞こえる」と「雑音が入って聞こえる」であった (図 5, 6)。

図 5 は難聴者との出会いの経験の有無と難聴の症状で音が「とぎれて聞こえる」というものがあると思うかどうかの関係を示したものである。難聴者との出会いの経験のある者は「とぎれて聞こえる」と答える者が 25.2% でない者のそれ (12.1%) より多かった。

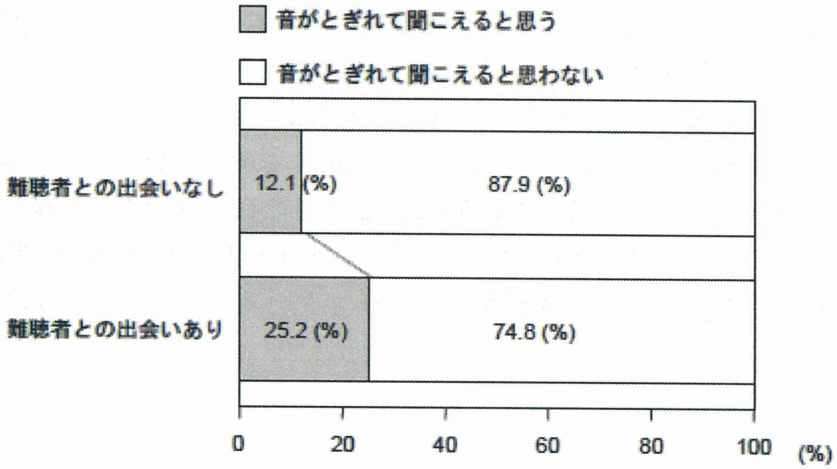

図 5. 難聴者との出会いの経験と「とぎれて聞こえる」症状への認識の関係

図 6 は難聴者との出会いの経験の有無と難聴の症状に「雑音が入って聞こえる」ものがあると思うかどうかの関係を示したものである。難聴者との出会いのある者は「雑音が入って聞こえる」と回答する者が 27.1% でない者のそれ (15.9%) より多かった。

全体的に認知度の低い 2 項目であったが、難聴者との関わりを持った者の方が難聴の症状について認識があると言える。

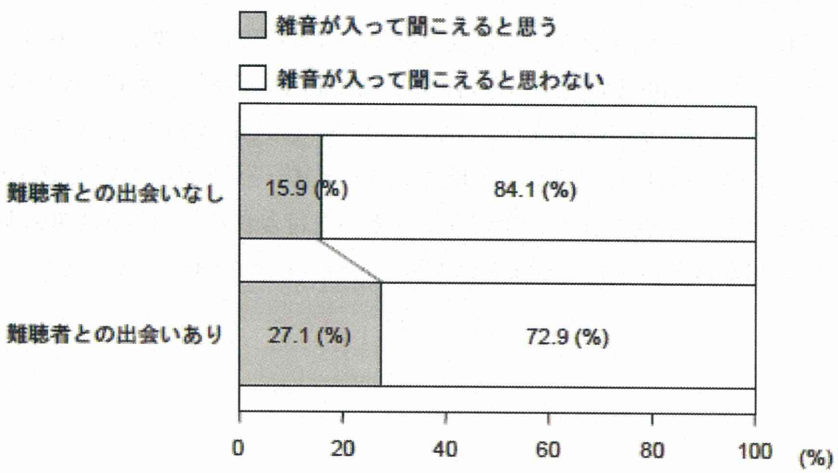

図 6. 難聴者との出会いの経験と「雑音が入って聞こえる」症状への認識の関係

(7) 補聴器の効果に対する認識

健聴者と難聴者とのコミュニケーションの上で関わりの深いものであると考え、健聴者の補聴器に対する認識について、「補聴器の効果はどのようなものであると思いますか。」という質問を行った。質問は項目の一つを選択させる形式で、回答は表 3 の通りである。

「音を大きくする効果」「音を鮮明にし、大きくする効果」を選択する者がともに 40% 前後みられ、補聴器は音を大きくするものであるという認識の強さが伺える。しかし、正解である「音を大きくする効果」と回答したものは 38.9% であり、残りの 61.1% の者は補聴器の効果に対して正しい理解をしていなかった。このことは難聴者とのコミュニケーションの上で重要な課題となると言える。

表 3. 健聴者が考える補聴器の効果

健聴者が考える補聴器の効果	人数 (人)	パーセント(%)
音を鮮明にし、大きくする効果	95	39.7
音を大きくする効果	93	38.9
音を鮮明にする効果	48	20.1
無回答	3	1.3

n = 239

(8) 聴覚障害者手帳を持つ人はどのくらいの聴力レベルだと思うか

「聴覚障害手帳の交付を受けている人はどの程度の大きさの音まで聞こえていると思いますか。」という質問を行った。紙面において音の大きさを選ばせるのは困難であるため、以下のように，目安としてそれぞれのデシベルを具体的な音に置き換えて選ばせた。呼吸音… 10 db、ささやき声… 20 db、新聞をめくる音…30 db、図書館での雑音… 50 db、普通の会話… 70 db、掃除機の音… 90 db、電車の通るガード下… 100 db、自動車のクラクション… 110 db。結果を表 4 に示す。

割合の高かったものは「掃除機の音までは聞こえる」28.2% と「普通の会話までは聞こえる」27.2% であった。障害者手帳 = 普通の生活に困る程度の者が交付される、という認識のあらわれとも考えられる。次いで割合の高かったものは「全て聞こえない」で 13.4% であった。

表 4. 健聴者の考える聴覚障害手帳の交付を受けている人の聴力レベル

聞こえる音の項目	人数 (人)	パーセント(%)
呼吸音まで	5	2.1
ささやき声まで	4	1.7
新聞をめくる音まで	21	8.8
図書館での雑音まで	20	8.4
普通の会話	65	27.2
掃除機の音まで	69	28.9
電車の通るガード下まで	18	7.5
クラクションまで	5	2.1
全て聞こえない	32	13.4

n = 239

(9) 聴覚障害を持つ者と健聴者が同じ学校で学ぶことについてどう思うか

「健聴者と聴覚障害者が同じ学校 (通常学校) で学ぶことについてお聞きします。健聴者の立場と聴覚障害者の立場の両方の立場になったつもりでお答え下さい。」という質問を行った。この質問は、(2) で「聴覚障害 (難聴) をもっている」と回答した者 (5 名) および「無し」と回答した者 (239 名) のそれぞれに、健聴者も難聴者も同じ学校で学ぶことに「賛成」、「反対」、「わからない」で答えてもらう形式で自由記述欄としてそれぞれの理由の欄を設けた。

[1] 「聴覚障害 (難聴) をもっている」と回答した者 (5 名) の意見

表 5. 健聴者の立場として

健聴者の立場として	人数 (人)	パーセント(%)
賛成	4	80.0
反対	0	0.0
わからない	1	20.0

賛成理由

- 聴覚障害を持っていてもほとんど普通の人とかわらないから。
- 聴覚障害者を受け入れる学校が少ない。
- 耳がきこえないからといって違う学校というのは…。

わからない理由

- 回答なし

表 6. 難聴者の立場として

難聴者の立場として	人数 (人)	パーセント(%)
賛成	3	60.0
反対	0	0.0
わからない	2	40.0

賛成理由

・聴覚障害を持っていても工夫次第で通常学校でも十分やれる自信があるから。

・聴覚障害者を受け入れる学校が少ない。

わからない理由

・同じ学校で学びたいけど周囲に迷惑をかけたくない。

[2] 「聴覚障害 (難聴) 無し」と回答した者 (239 名) の意見

「健聴者の立場として」は「賛成」が 59.4% と高く、「わからない」が 31.0% という結果になった。「難聴者の立場として」では「わからない」が 45.2% と一番高く、「賛成」が 30.1% 「反対」が 20.1% となり、「健聴者の立場として」回答した結果とはかなりの違いがみられた。

表 7. 健聴者の立場として

健聴者の立場として	人数 (人)	パーセント(%)
賛成	142	59.4
反対	19	7.9
わからない	74	31.0
無回答	4	1.7

表 8. 難聴者の立場として

難聴者の立場として	人数 (人)	パーセント(%)
賛成	72	30.1
反対	48	20.1
わからない	108	45.2
無回答	11	4.6

次に「健聴者の立場として」と「難聴者の立場として」でそれぞれの回答種類別にデータを処理した。その結果を表 8 に示す。この際、無回答であったものを除いて 225 名分を処理した。

表 9. 健聴者の回答

健聴者の立場として—難聴者の立場として	人数 (人)	パーセント(%)
賛成—賛成	56	24.9
賛成—反対	22	9.8
賛成—わからない	58	25.8
反対—賛成	4	1.8
反対—反対	14	6.2
反対—わからない	1	0.4
わからない—賛成	8	3.6
わからない—反対	12	5.3
わからない—わからない	50	22.2

この結果でも表 7 や表 8 の結果と同じく「健聴者として賛成だが難聴者の立場だったらわからない」という回答が最も多く 25.8% であった。次いで「どちらの立場としても賛成」が 24.9% 「どちらの立場としてもわからない」が 22.9% であった。「健聴者として反対」の項目にあてはまるものはいずれも割合が低い傾向がみられ、「難聴者の立場だったらわからない」の項目は割合が高い傾向がみられた。

(10) 難聴を抱える者が生活をする上であると良いと思う工夫や配慮 (聴覚障害を持っている人を対象に)

[1] 5 人の聴力レベルや装用器具について

A：ある一定の音域がきこえないが、実害がないため装用器具は使用していない。

B：両耳とも先天性難聴で、聴力レベルが低く人工内耳を装用している。

C：先天性難聴で障害者手帳 6 級。補聴器を装用している。

D：片耳が先天性難聴。片耳だけなので装用器具は使用していない。

E：両耳が後天性の感音性難聴で、人との会話に困るため補聴器を装用している。

[2] コミュニケーションをとるとき

・ゆっくり話して欲しい。

・何度も話を聞き返してしまう事を受け入れて欲しい。

・大きな声で話して欲しい。

・身ぶり、手ぶりがあると良い。

[3] 制度・法律について

・特に変えて欲しいものはない。

・補聴器等の器具に関する情報を、メガネやコンタクトレンズ並みに得られるようにして欲しい。

[4] 学校環境

・特に不便を感じた事はないが、授業の際に席を前の方にする配慮があると嬉しい。

・授業の時に先生の話がわかるような工夫をして欲しい。

[5] 公共の設備

・暗い夜道が恐いのでもっと道路を明るくして欲しい。

[6] 健聴者に伝えたいこと

・障害を持っていても感情やその他の中身は普通の人と同じなので、特別に接し方に気負わなくても大丈夫。

考察

新生児聴覚スクリーニングが普及してきたことにより、早期に難聴を発見できるようになってきた。そのため、幼児期の早い段階からその子どもにあった補聴器や人工内耳を装用する手段を選ぶことが可能になり、聴力の習得のみならず言語の習得もかなりのレベルまで可能になった。信州大学附属人工内耳センターでは、新生児聴覚スクリーニングから保護者や患児の支援、人工内耳のマッピング、(リ)ハビリテーションまで総括的に管理・支援を行っている。このような医療施設は増えつつあるが、まだまだ一般的に利用できるまで広がってはいない。いまだそのような医療施設の整っていない都道府県も数あるのが現状である。近くにそのような医療施設がないために、手段の選択肢を狭めてしまうこともありと推測される。一方、医療の発達に伴って難聴者の聴力レベルや言語獲得の能力は飛躍的に向上した。このことは医療の発達という視点では大変素晴らしい成果であるが、健聴者には難聴を抱えている事がわかりにくくなってきた。すなわち、補聴器の効果の限度である集音する角度や「はっきり聞こえない」という症状に対応しきれない面で「聞こえているはずなのに無視された」など誤解を受けやすくなっていることも難聴者の経験としてある。医療によって難聴者の従来の壁であった聴覚や言語そのもののQOLは目覚ましく向上してきているが、人々 (健聴者) からの認識はまだまだ十分とは言えず、対人関係等の社会的な面でのQOLは医療の発達だけでは解決しがたい問題だと考えられる。

一方、教育現場に関しては、医療に発達に伴う聴力レベルや言語習得レベルの向上により、難聴を抱える子どもたちの学習の場は、近年、聾学校 (特別支援学校) 以外にも広がっている。人工内耳センターの支援員の方も話されていたように、難聴児が健聴児と共に生活を送ることは言語能力の維持や向上の面で有益な事であるが、在籍児童数は聾学校 (特別支援学校) よりも通常学校の方が圧倒的に多いため、同世代の子どものモデルをより多く身近に置く事ができる。私はこのことを受けて健聴者側にも同じ事が言えると考えた。すなわち、近年、「インクルージョン教育」[2] という考えが注目されている。障害を持つ・持たないに関わらず、排除されるおそれのある多様なニーズをもつ全ての子どもを対象に通常学校の現場でそれぞれのニーズへ対応していくという考えのものである。この考えは排除されるおそれのある子どもも、そうでない子どもも皆一緒に学

ばせることによって対人関係を学ぶ機会や、障害を持つ子どもに関しては、その障害についての認識を深める等の機会になると考えられる。難聴児に置き換えると、通常学校に通う事によって、周りの子どもたちも学校生活や遊びの中で自ずと障害に関する認識が高まり、工夫を見出すことが出来るようになる機会になり得ると考えた。このことは学校就学世代である人格形成期の子どもたちにとって、とても意味のあることであると考えられる。

政権が自民党政権から民主党政権に代わったことに伴って、「障害者自立支援法」を廃止する宣言が平成 21 年 9 月になされた。平成 22 年 1 月現在は施行されているものの比較的新しく出来た法であった事やそれまでと制度が大きく変わった事から障害を持つ人々は動揺していることが推測される。「障害者福祉支援法」は、制定された当時から問題点は数多くあがっていたが、この法を廃止した後の代替の法律はどのようなものになるのか期待と不安を抱えていると思われる。聴覚障害者の障害者手帳の交付は 6 級から行われているが、その交付される聴力レベル (表 10) と本研究による調査結果 (表 4) はほとんど一致していた。健聴者の認識と難聴者の制度が一致しているという事は、健聴者が状況を想像して不便だろうと感じる境界と制度が一致しているということである。このことから、聴力レベルに関しての健聴者の認識は高いと思われる。

表 10. 聴覚障害の障害程度等級表

2 級	両耳の聴力レベルがそれぞれ 100 db 以上のもの
3 級	両耳の聴力レベルが 90 db 以上のもの (耳介に接しなければ大声語を理解し得ないもの)
4 級	1. 両耳の聴力レベルが 80 db 以上のもの (耳介に接しなければ話声語を理解し得ないもの) 2・両耳による普通話声の最良の語音明瞭度が 50%以下のもの
6 級	1. 両耳の聴力レベルが 70 db 以上のもの (40 センチメートル以上の距離で発声された話声語を理解し得ないもの) 2. 一個耳の聴力レベルが 90 db 以上、他側耳の聴力レベルが 50 db 以上のもの

※「身体障害者福祉法施行規則」[3] より抜粋

本研究による質問紙調査の結果からいくつかのことが明らかになった。第一に、健聴者の聴覚障害の症状のイメージのしにくさである。図 1 に示すように、「物が見えにくい状態 (視覚障害)」の方が「音が聞こえにくい状態 (聴覚障害)」よりも想像しやすいと考える健聴者が多いことが明らかになった。本研究では、大学生に対して調査を行ったため、健聴者の若い世代には聴覚障害が一般的にイメージしにくく、それと比較して物が見えづらい状態は視力低下という身近な現象に置き換えて想像しやすかったのではないかと思われる。聴力の低下も視力の低下と同じく老化に伴って発生していくものではあるため、対象をもう少し広げるとその結果も変わるかもしれない。第二に、健聴者の補聴器に関する認識である。補聴器には音を大きくする効果はあるが、音を鮮明にする働きはない。しかし、表 3 で示したように、不正解である「音を鮮明にする効果」や「音を鮮明にし、大きくする効果」を選択した者が全体の 61.1% を占めた。この認識の低さが難聴者の対人関係で

の QOL の低下や難聴者の悩みに深くかかわっていると考えられる。第三に、健聴者と難聴者が通常学校で共に学ぶ事についての認識である。この質問は健聴者に「健聴者の立場」と「難聴者の立場」の両方の立場になったつもりで回答してもらったが、「健聴者の立場」では賛成と答える者が 59.4% と多かった (表 7)。しかし、「難聴者の立場」ではわからないと答えた者が 45.2% にまで達した (表 8)。「賛成」の理由の内訳では「差別はよくない」や「一緒にいることで健聴者が学ぶ事があると思う」というものが多かった。「わからない」の理由の内訳では「障害の程度による」や「気を遣わせてしまうと思うと迷う」というものが多く見られた。この結果は、健聴者としての立場では一緒に難聴者と学ぶ事に関して肯定的だが、いざ、難聴者の立場になると消極的になる者が多いといくことであり、おそらく健聴者は難聴者と共に過ごすことに関しては特に気を遣うことはないが、難聴者の立場ではどういう事に困る可能性があるのかという事に対する認識があまりなく、想像しにくいというのではないかと考えられた。健聴者が持つ難聴という障害の状態に対する認識の程度はあまり高くないと考えられる。第 4 に、難聴者との出会いの経験と難聴への認識の関わりである。図 2 から図 4 に示すように、難聴者との出会いがない人は、出会いのある人と比較して、難聴者を「聞くことが出来ない」、「可哀想」、「手話を使う」と思う人が有意に多かった。おそらく出会いのあった者はある程度交流をしていたり、人工内耳や補聴器の存在を知っていたりしたためにこのような結果になったと推測される。特に、「聞くことが出来ない」と「手話を使う」というイメージは関連があり、聞くことができないから手話を使う、という連想がされやすいのではないかと思う。しかし、現実に手話を使う人はたくさんいるが、人工内耳や補聴器を幼いころから装用していた者は手話を使わない事も多く、そのイメージから「コミュニケーションがとりにくい」と思われてしまうもあると予想される。このことは難聴者にとって対人関係でのストレスになり得ると推測される。また、難聴の症状に対するイメージでも難聴者との出会いの経験の有無で有意差がみられた。「音が小さく聞こえる」、「ぼやけて聞こえる」、「とぎれて聞こえる」および「雑音が入って聞こえる」という項目の中で、「とぎれて聞こえる」と「雑音が入って聞こえる」の症状の認識が著しく低かった (表 2) が、それら 2 の認識については難聴者との出会いの経験の有無で有意差がみられた (図 5 および 6)。すなわち、難聴者との出会いの経験がある者ほど「とぎれて聞こえる」や「雑音が入って聞こえる」の症状への認識が高い傾向になり、難聴者との出会いの経験がある者の方が、難聴や難聴者に関する認識が高い事が推測される。

本研究では、養護教諭という立場から、難聴者やその保護者の QOL を向上させるためには学校教育でどのような働きかけができるか、学校という場を難聴者と健聴者の認識の差を埋める場としてどのように活用していけるのかを考察することを目的として、難聴者とその家族が抱える悩みや想いと、健聴者の認識の差はどこにあるのか、差が出来てしまう原因はどこにあるのかを明らかにしてきた。難聴者を取り巻く様々な要素について、難聴者の QOL を高める視点には医療、教育、福祉・移行支援など様々なものがあり、それぞれがそれぞれの視点から難聴者の QOL を高めているが、最終的に QOL を高める根本的な要素は「人」である。人々の認識が医療を高めたり、教育方法を考えたり、福祉・支援を充実させようとする。また、難聴者に関わる健聴者 (学校等での友人や、社会生活上での接点を持つ全ての人) が難聴者や難聴への理解があると、難聴者にとって対人関係の面でも充実し得る。難聴者にとってよりよい社会を作り出すためには、前述してきたような難聴者の悩みと健聴者の認識の差を埋めていく事が必須である。教育の面でそのことを考えた時

に、学校を難聴者の悩みと健聴者の認識の差を埋める場としてもっと活用できるのではないかと考えられる。本研究では、難聴者との出会いの経験が難聴者への正しい理解につながっていることを示した。従って、人格形成期である就学世代に難聴を抱える子どもたちと健聴児を一緒に学ばせる事は一つの方法として大変重要であると考えられる。子どもたちは人格形成期にいろんなモデルを見たり接したりする事で様々な事に理解をしていくため、最初は「知らなかった人・事」や「身近でなかった人・事」であっても、人格形成期にある子どもたちはだんだんと日常化していくのである。この日常化とは、単なる「慣れ」というものではなく、遊びや生活での経験を通して障害自体に対する認識やそれを抱える人に対する認識が自然に高まることによって身近な事とされるという意味である。人格形成期に様々な出会いをすることは、大人になってから同じような出会いがあった時にすんなりと関係を築く事が可能であると考えられる。学校とはそのような「出会い」を経験させる場であり、その「出会い」を有意義なものにさせるのは教職員をはじめとする学校組織である。養護教諭は、「人」の融合・調和を図る点で「出会い」を難聴児と健聴児双方にとって有意義なものとする為のサポートする必要があり、そのためには難聴を抱える人々の背景にある様々な要素を理解し、その様々な要素 (機関) の環に入り連携していく事が大切である。それと同時に、学校の機関の中で難聴児と健聴児が共に楽しく活躍でき、学びあえるような学校生活や行事等をコーディネートする役割を積極的に担うことも重要である。学校現場では、難聴児の受け入れ態勢や周囲の子どもたちへの教育、教職員の知識の向上などの支援態勢を整えている最中ではあるが、本研究の成果をもとに、養護教諭は様々な現状を把握してその専門性を活かして出来る事を日々考える必要がある。

謝辞

本稿をまとめるにあって、ご協力くだった先生方や学生の皆様に心より感謝の気持ちを申し上げます。本研究は、茨城大学 教育学部 研究費特別配分の助成を受けて実施しました。

注

1) 宇佐美真一 (編著).『きこえと遺伝子』 (金原出版). 2006.
2) 荒川智. 『インクルーシブ教育入門 - すべての子どもの学習参加を保障する学校・地域づくり』(クリエイツかもがわ). 2008.
3) 身体障害者福祉法施行規則
(http://law.e-gov.go.jp/cgi-bin/idxselect.cgi?IDX_OPT=5&H_NAME=&H_NAME_YOMI=%82%A0&H_NO_GENGO=H&H_NO_YEAR=&H_NO_TYPE=2&H_NO_NO=&H_FILE_NAME=S25F03601000015&H_RYAKU=1&H_CTG=1&H_YOMI_GUN=1&H_CTG_GUN=1)

Piezoelectric materials mimic the function of the cochlear sensory epithelium

Takatoshi Inaoka[a,1], Hirofumi Shintaku[b,1], Takayuki Nakagawa[a,2], Satoyuki Kawano[b], Hideaki Ogita[a], Tatsunori Sakamoto[a], Shinji Hamanishi[c], Hiroshi Wada[d], and Juichi Ito[a]

[a]Department of Otolaryngology, Head and Neck Surgery, Graduate School of Medicine, Kyoto University, Kyoto 606-8507, Japan; [b]Department of Mechanical Science and Bioengineering, Graduate School of Engineering Science, Osaka University, Osaka 560-8531, Japan; [c]Department of Mechanical Engineering, Sendai National College of Technology, Miyagi 981-1239, Japan; and [d]Department of Bioengineering and Robotics, Graduate School of Engineering, Tohoku University, Miyagi 980-8579, Japan

Edited by Dale Purves, Duke University Medical Center, Durham, NC, and approved September 13, 2011 (received for review June 25, 2011)

Cochlear hair cells convert sound vibration into electrical potential, and loss of these cells diminishes auditory function. In response to mechanical stimuli, piezoelectric materials generate electricity, suggesting that they could be used in place of hair cells to create an artificial cochlear epithelium. Here, we report that a piezoelectric membrane generated electrical potentials in response to sound stimuli that were able to induce auditory brainstem responses in deafened guinea pigs, indicating its capacity to mimic basilar membrane function. In addition, sound stimuli were transmitted through the external auditory canal to a piezoelectric membrane implanted in the cochlea, inducing it to vibrate. The application of sound to the middle ear ossicle induced voltage output from the implanted piezoelectric membrane. These findings establish the fundamental principles for the development of hearing devices using piezoelectric materials, although there are many problems to be overcome before practical application.

cochlear implant | hearing loss | mechanoelectrical transduction | traveling wave | regeneration

The cochlea is responsible for auditory signal transduction in the auditory system. It responds to sound-induced vibrations and converts these mechanical signals into electrical impulses, which stimulate the auditory primary neurons. The human cochlea operates over a three-decade frequency band from 20 Hz to 20 kHz, covers a 120-dB dynamic range, and can distinguish tones that differ by <0.5% in frequency (1). It is relatively small, occupying a volume of <1 cm^3, and it requires ~14 μW power to function (2).

The mammalian ear is composed of three parts: the outer, middle, and inner ears (Fig. 1*A*) (3). The outer ear collects sound and funnels it through the external auditory canal to the tympanic membrane. The cochlea consists of three compartments: scala vestibuli and scala tympani, which are filled with perilymph fluid, and scala media, which is filled with endolymph fluid (Fig. 1*C*). The scala vestibuli and scala tympani form a continuous duct that opens onto the middle ear through the oval and round windows. The stapes, an ossicle in the middle ear, is directly coupled to the oval window. Sound vibration is transmitted from the ossicles to the cochlear fluids through the oval window as a pressure wave that travels from the base to the apex of the scala vestibuli through the scala tympani and finally to the round window (Fig. 1*B*). The scala media are membranous ducts that are separated from the scala vestibuli by Reissner's membrane and separated from the scala tympani by the basilar membrane. The pressure wave propagated by the vibration of the stapes footplate causes oscillatory motion of the basilar membrane, where the organ of Corti is located. The organ of Corti contains the sensory cells of the auditory system; they are known as hair cells, because tufts of stereocilia protrude from their apical surfaces (Fig. 1*D*). The oscillatory motion of the basilar membrane results in the shear motion of the stereociliary bundle of hair cells, resulting in depolarization of hair cells.

The cochlea amplifies and filters sound vibration by means of structural elements, especially the basilar membrane, and through an energy-dependent active process of fine-tuning that is largely dependent on the function of the outer hair cells. The location of the largest vibration in the basilar membrane depends on the frequency of the traveling wave (Fig. 1*E*) (4, 5). The width, thickness, and stiffness of the basilar membrane vary along the length of the cochlear spiral. Because of this variation in mechanical impedance, high-frequency sounds amplify the motion of the basilar membrane near the base of the cochlea, whereas low-frequency sounds amplify its motion near the apex (Fig. 1*E*). Hair cells within a frequency-specific region are selectively stimulated by basilar membrane vibration according to the traveling wave theory. The mechanical filtering of sound frequency by structural elements of the cochlea allows it to function as a highly sophisticated sensor. Additional details of cochlear macro- and micromechanics can be found in the review by Patuzzi (6).

Both inner and outer hair cells are arranged in four rows along the entire length of the cochlear coil (Fig. 1*D*). The single row of inner hair cells plays a central role in transmission of sound stimuli to the auditory primary neurons, whereas the three rows of outer hair cells amplify and filter sound vibration. The outer hair cells are capable of somatic electromotility driven by the molecular motor protein prestin, which is located in the outer hair cell membrane (7). The electromotility of outer hair cells contributes to the fine-tuning to sound frequency (8–11). The stereocilia also play a role in signal amplification in amphibians. Active hair bundle motions correlated with transduction channel gating resonate with the stimulus and enhance basilar membrane movement. A more detailed description of the mechanisms of cochlear amplification can be found in the review by LeMasurier and Gillespie (12).

Sensorineural hearing loss (SNHL) is a common disability caused by loss of hair cells (13, 14). Most cases of SNHL are irreversible, because mammalian hair cells have a limited capacity for regeneration (15, 16). The loss of outer hair cells diminishes the fine-tuning of the cochlea to sound frequency. The loss of inner hair cells results in profound hearing impairment because of lack of transmission of auditory signals from the cochlea to the central auditory system. At present, therapeutic options for profound SNHL are limited to cochlear implants, which have partially restored the hearing of more than 120,000 patients worldwide (17). A cochlear implant has both external and internal parts. The former includes microphones, speech processors, and transmitters, and the latter includes receivers,

Author contributions: H.S., T.N., S.K., T.S., H.W., and J.I. designed research; T.I., H.S., H.O., and S.H. performed research; H.O., S.H., and H.W. contributed new reagents/analytic tools; T.I., H.S., T.N., S.K., T.S., and S.H. analyzed data; and T.I., H.S., and T.N. wrote the paper.

The authors declare no conflict of interest.

This article is a PNAS Direct Submission.

Freely available online through the PNAS open access option.

[1]T.I. and H.S. contributed equally to this work.

[2]To whom correspondence should be addressed. E-mail: tnakagawa@ent.kuhp.kyoto-u.ac.jp.

This article contains supporting information online at www.pnas.org/lookup/suppl/doi:10.1073/pnas.1110036108/-/DCSupplemental.

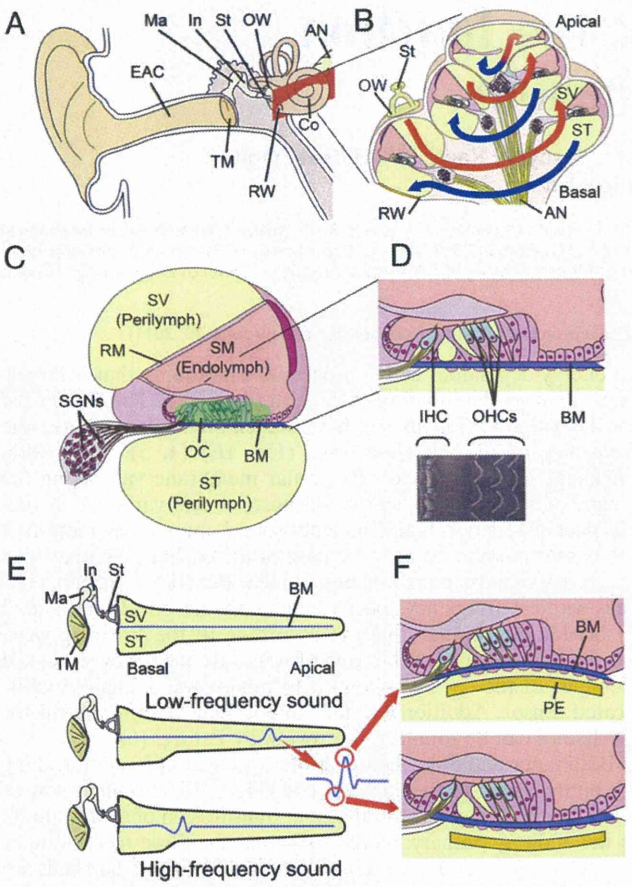

Fig. 1. Anatomy of the mammalian cochlea. (*A*) Schematic drawing of the human auditory system. AN, auditory nerve; Co, cochlea; EAC, external auditory canal; In, incus; Ma, malleus; OW, oval window; RW, round window; St, stapes; TM, tympanic membrane. (*B*) Schematic drawing of a cochlear coil. Sound vibrations transmitted to the cochlea fluid in the scala vestibule (SV) through the OW travel up from the basal turn to the apical turn (red lines) and then back to the basal turn (blue lines) in the scala tympani (ST). (*C*) Schematic drawing of a cochlear duct. The ST and SV are filled with the perilymph. The scala media (SM), which is separated from the ST by Reissner's membrane (RM) and separated from the ST by the basilar membrane (BM), is filled with the endolymph. The organ of Corti (OC) is located on the BM. Spiral ganglion neurons (SGNs) are located in the modiolus of the cochlea. (*D*) Schematic drawing and scanning EM of the organ of Corti. One row of inner hair cells (IHCs) and three rows of outer hair cells (OHCs) are arranged along the entire length of the cochlear coil. (*E*) Schematic drawing of traveling wave theory. Low-frequency sounds vibrate the BM in the apical portion of a cochlea, whereas high-frequency sounds provoke vibration in the basal portion of a cochlea. (*F*) Schematic drawing showing the vibration of the BM and a piezoelectric membrane (PE) implanted in the ST of a cochlea in response to sound stimuli.

stimulators, and electrode arrays, which are surgically inserted under the skin or into the cochlea. Arrays of up to 24 electrodes are generally implanted into the scala tympani, and they directly stimulate the auditory primary neurons. The conversion of sound stimuli to electrical signals is performed by the external speech processor and transmitter and the internal receiver and stimulator. A battery is required to generate electrical output. Schematics and additional descriptions of the history, present status, and future directions of cochlear implants can be found in the work by Zeng et al. (17).

The traveling wave theory proposed by von Békésy (4, 5) was validated using cochleae from cadavers, indicating that, even after complete loss of hair cell function, the mechanical tonotopy for sound frequency remains within the cochlea. This phenomenon also persists in deafened cochleae. However, to our knowledge, electrical hearing devices have not yet used mechanical cochlear tonotopy for sound frequency. In theory, an implantable device that converts sound vibration to electric potential could be fabricated using microelectromechanical systems and implanted close to the basilar membrane of the cochlea. The vibration of the basilar membrane in response to sound stimuli should be transmitted to the implanted device, generating an electrical output (Fig. 1*F*). According to the traveling wave theory, tuning for sound frequency should be determined largely by where the device is implanted.

To test this hypothesis, we developed a prototype artificial cochlear epithelium using a piezoelectric membrane, which functions as a sensor with the capability for acoustic/electric conversion without a battery (18). The piezoelectric device, although not life-sized, showed a tonotopic map for frequencies of 6.6–19.8 kHz in air and 1.4–4.9 kHz in silicone oil, and it generated maximum electrical output from an electrode placed at the site of maximum vibration. In the present study, we showed that the electrical output from a prototype device in response to sound stimuli induced auditory brain-stem responses (ABRs) in deafened guinea pigs. We fabricated a life-sized device using microelectromechanical systems and tested its responses to sound application when implanted in the guinea pig cochlea. Our findings are a major step to developing an implantable artificial cochlear epithelium that can restore hearing.

Results and Discussion

Effects of Kanamycin and Ethacrynic Acid on Auditory Primary Neurons and Hair Cells. To examine the potential of a piezoelectric device to induce biological ABRs in deafened guinea pigs, we established a model in which all hair cells were lost but auditory primary neurons remained to avoid the confounding effects of hair cell-mediated responses. Adult Hartley guinea pigs ($n = 6$) were administered an i.m. injection of kanamycin (KM; 800 mg/kg) followed by an i.v. injection of ethacrynic acid (EA; 80 mg/kg), and the compound action potential was measured to monitor hearing function. A total loss of hearing was observed 7 d after the administration of drugs in all animals at all tested frequencies. We then examined the thresholds of electrically evoked ABRs (eABRs), which are generated by direct electrical stimulation of the auditory primary neurons to determine the survival of these cells in the animal model. Measurements of eABR showed no significant elevation of eABR thresholds in animals treated with KM and EA compared with normal animals (2.50 ± 0.50 V in normal animals, 2.83 ± 0.37 V in test animals). Histological analysis revealed no significant loss of spiral ganglion, whereas there was a total of loss of hair cells in test animals (Fig. S1).

Generation of ABRs by a Piezoelectric Device in Living Guinea Pigs. A prototype piezoelectric device (Fig. 2*A*) containing a PVDF membrane (40-μm thickness) was fabricated using microelectromechanical systems as described previously (18). The piezoelectric membrane was used as a transducer, and its electrical outputs were amplified by 1,000-fold. For stimulation of auditory primary neurons, platinum–iridium ball electrodes were implanted into the scala tympani of the cochlear basal turn (Fig. 2*B*). Typical ABRs in response to increased acoustic stimuli were recorded in our model animals (Fig. 2*C*).

When acoustic stimuli of 104.4 dB sound pressure level (SPL) were applied to the piezoelectric membrane, the first positive wave of ABRs was clearly identified at a latency of 1.07 ± 0.05 ms (Fig. 2*C*), which was identical to the latency of the first positive wave in eABRs (0.98 ± 0.06 ms) in guinea pigs in the present study (Fig. S2). In general, the first wave of eABRs corresponds to wave II of normal ABRs (19). Compared with the latency of wave II of normal ABRs in normal guinea pigs ($n = 4$, 2.99 ± 0.11 ms) (Fig. S2), the latency of the first positive wave of piezoelectric device-induced ABRs was ~2 ms short. However, the latency of the first positive wave of piezoelectric device-

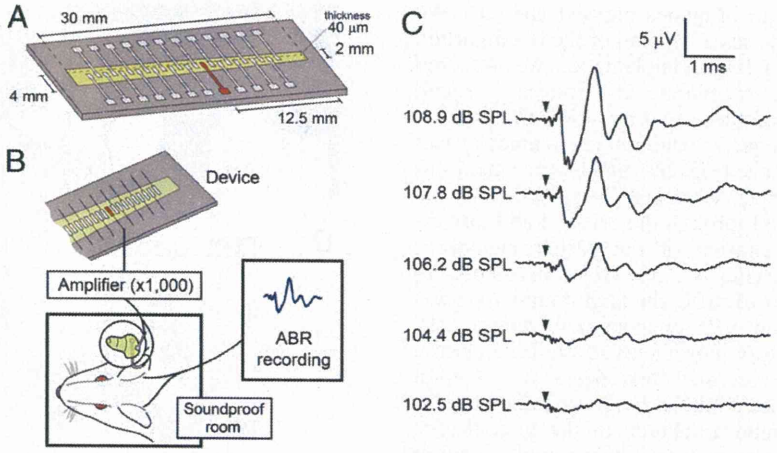

Fig. 2. ABR recording using a prototype device. (*A*) Schematic drawing of a prototype device with a piezoelectric membrane (yellow). A piezoelectric membrane has a thickness of 40 μm and a length of 30 mm. An array of 24 electrodes, made of aluminum thin film, is fabricated on the upper side of a piezoelectric membrane, which is aligned in the midline of the trapezoidal slit of the stainless plate. An electrode used in the experiment of stimulating auditory primary neurons is located 12.5 mm from the shorter side of the trapezoidal membrane (shown in red). (*B*) Schematic drawing of a setting for ABR recording using a piezoelectric device. Electrical signals generated by a piezoelectric membrane in response to acoustic stimuli are amplified and transferred to the cochlea. Bioelectrical signals were recorded as ABRs from needle electrodes inserted dorsal to ears. (*C*) ABRs by electrical signals derived from a prototype device by acoustic stimuli. Arrowheads indicate the timing of acoustic stimuli.

induced ABRs was almost similar to the latency between waves I and II of normal ABRs (0.83 ± 0.04 ms). These findings showed that the piezoelectric membrane generated biological ABRs by converting acoustic stimuli to electrical signals.

Transmission of Sound Vibration from the External Auditory Canal to the Implanted Piezoelectric Device. The transmission of sound waves from the external auditory canal to a piezoelectric membrane implanted into the cochlea is crucial to realize hearing recovery by a piezoelectric device based on the traveling wave theory. To test the transmission of sound waves from the external auditory canal to a piezoelectric membrane, we developed an implantable device that was specialized for the basal turn of the guinea pig cochlea (Fig. 3 *A* and *B*). The device contained a PVDF fluoride trifluoroethylene [P(VDF-TrFE)] membrane with a frequency response of 16–32 kHz, which corresponded to

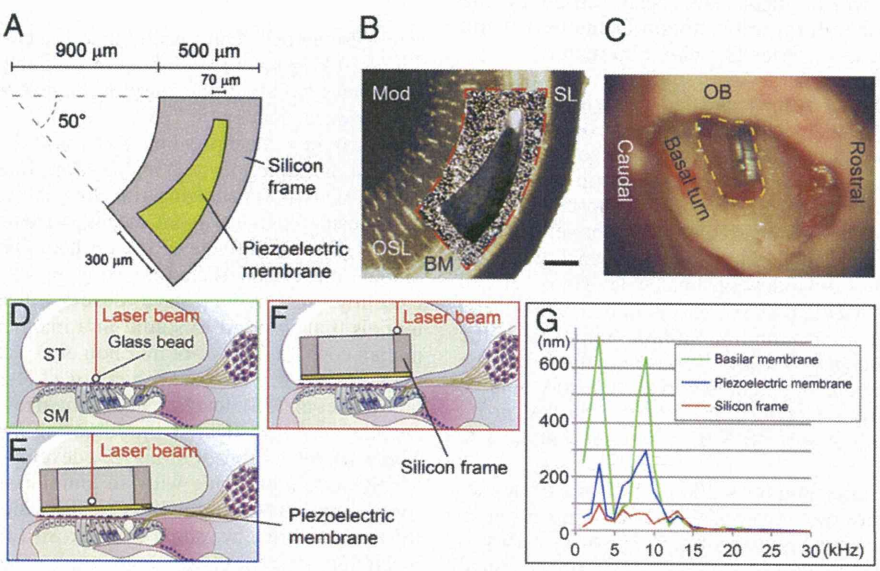

Fig. 3. Sound transmission from the external auditory canal to a piezoelectric device implanted in the cochlea. (*A*) Design of an implantable piezoelectric device. (*B*) A merged image of an implantable piezoelectric device and the basal turn of the guinea pig cochlea. To determine the radius of curvature of the outer border and the inner border of the fan-shaped silicon frame and location of the slit in the silicon frame, we measured radius of curvature of the cochlear basal turn, length between an inner edge of the spiral ligament (SL) and a medial end of the osseous lamina (OSL) where the device will be implanted, and length of the basilar membrane (BM; length between inner edge of spiral ligament and lateral end of osseous lamina). An outline of the silicon frame is shown by a red dotted line. The silicon frame is positioned on the osseous spiral lamina, and the slit of the device is located adjacent to the BM. Mod, cochlear modiolus. (Scale bar: 200 μm.) (*C*) A microscopic view of an implanted device in the basal turn of the guinea pig cochlea. The yellow dotted line indicates an opening in the basal turn of the cochlea. OB, otic bulla. (*D–F*) Schematic drawings of measuring vibration amplitudes using a laser Doppler vibrometer. A glass bead is placed on the BM (*D*), piezoelectric membrane (*E*), or silicon frame (*F*). Red lines indicate a laser beam from a laser Doppler vibrometer. SM, scala media; ST, scala tympani. (*G*) Vibration amplitudes of a BM (green), piezoelectric membrane (blue), and silicon frame (red) corresponding to frequencies of applied sounds.

the response of the basal turn of guinea pig cochleae (20). We implanted the device into the scala tympani of the basal portion of an intact cochlea (Fig. 3*C*). Before implantation, we measured the vibration of the basilar membrane in response to sound stimuli from the external auditory canal at various frequencies between 1 and 30 kHz. A glass bead (50-μm diameter) was placed on the basilar membrane (Fig. 3*D*), and its movement was measured using a laser Doppler vibrometer (21). When continuous pure tones were applied through the external auditory canal, the amplitudes for vibration of the basilar membrane showed peaks at 3 and 9 kHz (Fig. 3*G*, green line). In response to 3 kHz sound stimuli at 101.7 dB SPL, the largest amplitude was 642 nm, which was consistent with previous observations (21). Measurements of the vibratory movements of the piezoelectric membrane (Fig. 3*E*) also revealed two peaks of vibration amplitudes similar to the peaks of the basilar membrane (Fig. 3*G*, blue line). The maximum amplitude of the piezoelectric membrane was 293 nm in response to 9 kHz sound stimuli at 109.2 dB SPL.

In contrast to the piezoelectric membrane, measurements of the movements of the silicon frame (Fig. 3*F*) revealed no apparent peaks in the amplitudes of oscillations, which were all within 100 nm (Fig. 3*G*, red line). The differences in response between the piezoelectric membrane and silicon frame may be caused by the difference in the stiffness. In addition, the piezoelectric membrane was located closer to the basilar membrane than the silicon frame, and the basilar membrane may be a preferable location to receive sound vibration. These findings showed that sound stimuli transmitted through the external auditory canal caused vibration of a piezoelectric membrane implanted within the scala tympani of cochleae. Notably, the piezoelectric membrane exhibited similar tuning for sound frequency as the basilar membrane, indicating that it could reproduce the mechanical tonotopy of the latter. The tuning for sound frequency of the basilar and piezoelectric membranes differed from the tuning of the basilar membrane in normal guinea pig cochleae, which might have been caused by the opening of the cochlear wall for implantation of the device and taking measurements using a laser Doppler vibrometer.

Generation of Voltage Output by the Implanted Device in Response to Sound Stimuli. To show the technical feasibility of the piezoelectric hearing device, we examined whether sound stimuli generated electrical output from the piezoelectric membrane after implantation into the cochlea. For this purpose, we established an ex vivo model of a guinea pig temporal bone, in which sound stimuli were directly applied to the stapes, which transmits sound vibration to the oval window of the cochlea (Fig. 1 *A* and *B*). A miniaturized device modified to contain a silicon rod carrying electrodes for monitoring the voltage output from the piezoelectric membrane (Fig. 4 *A* and *B*) was implanted into the basal portion of cochleae. A miniaturized device was able to generate electrical output ranging from 0.14 to 5.88 mV in response to sound stimuli at 100 dB SPL at frequencies of 1–40 kHz in air (Fig. S3).

When 30-cycle tone-burst stimuli at 100 dB SPL at a frequency of 5, 10, or 20 kHz were directly applied to the stapes using an actuator, peak to peak voltage output of 23.7, 5.7, or 29.3 μV was recorded, respectively (Fig. 4*C*). After completion of the sound application, the amplitudes of voltage output gradually decreased and returned to the original level within 3 ms, which mimicked the biological response of the basilar membrane. In a control setting, in which an actuator generated sound stimuli but was not attached to the stapes, negligible voltage output was recorded (Fig. 4*C*). These findings showed that sound stimuli from the stapes generated voltage output from the piezoelectric device implanted in the cochlea. Notably, the voltage outputs from the piezoelectric device differed depending on the applied

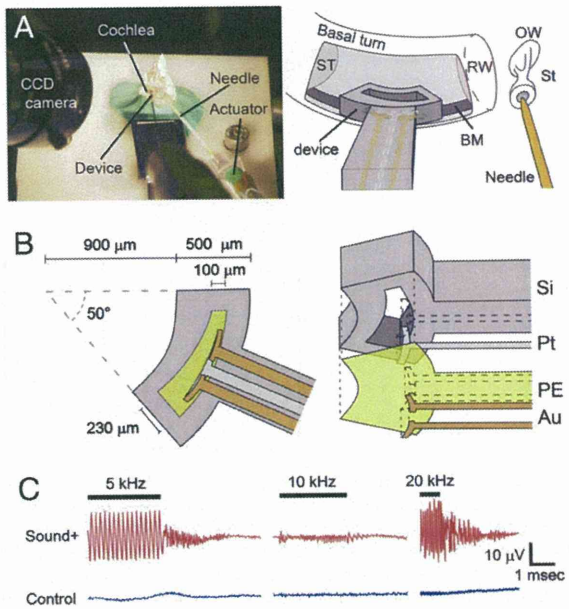

Fig. 4. Electrical output from the piezoelectric membrane implanted in the guinea pig cochlea in response to sound application to the stapes. (*A*) Photograph and schematic drawing showing the setting of an ex vivo system. A guinea pig temporal bone was set on a stage, and an implantable device was inserted into the scala tympani (ST) of the basal turn and placed close to the basilar membrane (BM). A needle was attached on the head of the stapes (St) to transmit sound vibrations through the oval window (OW). RW, round window. (*B*) Design of the implantable piezoelectric device. Au, gold film electrode; PE, piezoelectric membrane; Pt, platinum film electrode; Si, silicon frame. (*C*) Electrical output from a piezoelectric membrane in response to sound stimuli. Bars indicate the period for sound application. Waveforms in red show electrical output when sound stimuli are applied to the stapes, and waveforms in blue show those in a control setting.

sound frequency. The maximum voltage outputs in response to 5 and 20 kHz sound stimuli were similar (23.7 and 29.3 μV, respectively), whereas the outputs in response to 10 kHz sound stimuli were smaller (5.7 μV).

Researchers have previously attempted to develop an artificial cochlea that functions as a highly sophisticated sensor. Studies by von Békésy (4, 5) showing traveling waves in the basilar membrane using cochleae from cadavers led to the development of several physical models of the cochlea. The first group of these models comprised scaled-up versions of the cochlea (22–24). Recently, researchers have developed fluid-filled microscale models that respond to sound in a manner similar to the mammalian cochlea. The work by Zhou et al. (25) showed a tonotopic map over the 0.3- to 15-kHz band in a life-sized model. The work by Chen et al. (26) developed a beam array fixed on a trapezoidal channel and investigated the vibrating characteristics in water. The work by Wittbrodt et al. (27) developed a device containing a polyimide membrane with an aluminum frame, which shared some similarities with the biological cochlea in terms of traveling waves. The work by White and Grosh (28) used silicon micromachining technology to create their cochlea model. This work was important, because the batch micromachining process used to fabricate this system paved the way for the future integration of sensing elements into the structure to produce low-power, micromechanical, and cochlear-type sensor filters. However, these devices have no potential for generating electrical output in response to sound stimuli. Providing high-quality hearing through the cochlear implant involves the development of a device with high channel capability, low-power requirements, and small size (29). The work by Bachman et al. (29) fabricated

a micromechanical multiband transducer that consisted of an array of micromachined polymer resonators, and it examined its sensitivity to sound frequency; however, the work focused on the low-power requirements of the transducer and proposed a design that could be implanted into the middle ear cavity (29), which fundamentally differed from our concept.

The present report describes a device at the technology–biology interface that can mimic the function of the basilar membrane and inner hair cells using a combination of traditional traveling wave theory and microelectromechanical systems. This device could be described as the technological regeneration of hair cells. The device, which consists of a piezoelectric membrane and silicon frame, can be implanted into the guinea pig cochlea. It is able to resonate in response to sound stimuli similar to the natural basilar membrane and generate electric output, whereas previously reported devices required an electrical supply, and realizing low-energy requirements remains a goal for the future development of cochlear implants (29). We, therefore, consider the ability of our device to generate electrical output in response to sound stimuli to be a great advantage. In practice, the electrical output from our device is not sufficient to stimulate auditory primary neurons. The electrical output should be 10^5-fold higher than the output of the present device for effective stimulation of auditory primary neurons when electrodes are placed in the scala tympani similar to conventional cochlear implants. We should optimize the location and fixation of a piezoelectric device in a cochlea for obtaining the maximum oscillation of a piezoelectric membrane, because electrical output from a piezoelectric membrane after implantation in a cochlea decreased to ~10% of electrical output recorded in the in vitro setting (Fig. S3). To increase the power of a piezoelectric device, we will examine the potential of other piezoelectric materials for generation of electrical output and the effects of reduction in thickness of a piezoelectric membrane and multilayer constructions of piezoelectric membranes. In addition, it is also important to reduce electrical output required for sufficient stimulation of auditory primary neurons. For this purpose, we are developing microelectrodes that are able to access close to auditory primary neurons. Finally, our device has only passive sensitivity to sound frequencies. To enhance this sensitivity, additional mechanisms mimicking the function of outer hair cells need to be developed.

Materials and Methods

Experimental Animals. A total of 26 female adult Hartley guinea pigs (4–10 wk, 300–600 g in weight; Japan SLC) with a normal Preyer pinna reflex served as the experimental animals. Animal care was conducted under the supervision of the Institute of Laboratory Animals, Graduate School of Medicine, Kyoto University, Japan. All experimental procedures followed the National Institutes of Health Guidelines for the Care and Use of Laboratory Animals. In all procedures necessitating general anesthesia, the animals were administered an i.m. injection of midazolam (10 mg/kg; Astellas Pharma) and xylazine (0.01 mg/kg; Bayer). Supplemental doses were administered every 2 h or more often if the animal withdrew its leg in response to applied pressure.

eABR Recording. Measurements of eABRs were performed as previously described (30). Biphasic voltage pulses were generated under computer control using a real-time processor (Tucker-Davis Technologies). Electrical stimuli were applied between two intracochlear platinum–iridium electrodes. Bioelectrical signals were digitally amplified, averaged for 500 repetitions, and recorded using subdermal stainless steel needle electrodes.

Prototype Piezoelectric Device. The prototype piezoelectric device was fabricated as previously described (18). A thin aluminum film was formed on both sides of the 40-μm-thick PVDF membrane by sputtering. An electrode array with 24 rectangular elements was fabricated from the aluminum film using a standard photolithography and etching process on the upper side of the PVDF membrane. The aluminum film on the lower side served as a ground electrode.

Prototype Device ABRs. The ABRs produced using the prototype device were measured 7 d after the administration of KM and EA. The generation of trigger signals and the recordings of the evoked potentials were performed using PowerLab/4sp. The trigger signals were conveyed to a function generator (WF1945B; NF Corporation), which was programmed to generate a sinusoidal output signal for each trigger. The amplitudes and frequencies of the sinusoidal outputs were digitally controlled at a base frequency and duration of 5 kHz and 0.2 ms, respectively. The output signals were connected to a custom-made actuator, which delivered acoustic waves to the device. The amplitudes applied to the actuator were calibrated to produce vibrations of the piezoelectric membrane of the device equivalent to those vibrations produced by the application of sound at pressure levels ranging from 87 to 115 dB SPL. The electrical signals generated by the prototype device in response to the acoustic waves of the actuator were transmitted to a custom-made amplifier, which produced a 1,000-fold increase, and their waveforms and amplitudes were monitored by an oscilloscope (WaveJet 314A; LeCroy). A biphasic signal was extracted from the electrical signals using a custom-made complementary metal oxide semiconductor switch to prevent the signal induced by reverberation of the piezoelectric membrane. Signals from the complementary metal oxide semiconductor switch were also conducted to platinum–iridium electrodes implanted in the scala tympani of the cochlear basal turn of guinea pigs (n = 4) placed in a soundproof room. The bioelectrical signals were averaged for 500 repetitions, and they were recorded using subdermal stainless steel needle electrodes. The responses were verified at least two times.

Implantable Miniaturized Device. An implantable device for examining the transmission of sound from the external auditory canal to the piezoelectric membrane was fabricated using a P(VDF-TrFE) membrane (KF-W#2200; Kureha) and a silicon frame according to the methods described previously (31). The surface of the 300-μm-thick silicon substrate (100) was penetrated by hexamethyldisilazane (Tokyo Ohka Kogyo) to enhance adhesion of the P(VDF-TrFE) membrane. An *N,N*-dimethylformamide (Nacalai Tesque) solution containing P(VDF-TrFE) at a concentration of 8% weight was spun on the silicon substrate. It was then heated to crystallize the P(VDF-TrFE) at a thickness of 3 μm. The opposite side of the silicon substrate was treated with photolithography and an etching process to form a fan-shaped silicon frame with a slit to accommodate the flexible piezoelectric membrane. The fan-shaped silicon frame and the location of the slit were designed based on the shape of the cochlear basal turn of adult guinea pigs. The slit in the silicon frame was positioned such that the sheet was adjacent to the portions of the basilar membrane where it vibrated the most (32).

Surgical Procedure for Implantation of the Miniaturized Device into the Cochlea. A laser Doppler vibrometer (LV-1100; Ono Sokki) was used to measure the vibrations of the basilar membrane and the piezoelectric membrane of the device implanted in the cochlea. Under general anesthesia, a retroauricular incision was made to expose the bulla of an experimental animal with a normal cochlea (n = 1). An opening was made in the otic bulla while preserving the tympanic annulus, tympanic membrane, and ossicles. This opening was used to direct the laser beam to the cochlea to measure the vibrations. After a skin incision in the submandibular region, cochleostomy was made in the scala tympani of the basal turn for insertion of the implantable device. After a tracheotomy, suxamethonium chloride hydrate (10 mg; Kyorin Pharmaceutical) was injected i.m., and a ventilation tube was inserted into the trachea to suppress movements from spontaneous ventilation.

Measurement of Vibrations Using a Laser Doppler Vibrometer. Sine wave signals produced by a function generator were delivered to an electrostatic speaker driver (ED1; Tucker-Davis Technologies) to generate pure tones from an electrostatic speaker as acoustic stimuli. Continuous pure tones were applied through the external auditory canal of the animals from 1 to 30 kHz at 1-kHz intervals at levels between 62.5 and 109.2 dB SPL. We measured the vibrations in response to sound stimuli using a laser Doppler vibrometer (21, 33). Initially, a glass bead (50-μm diameter) was set on the basilar membrane. A laser Doppler vibrometer beam was directed to the glass bead (Fig. 3). The vibrations of the basilar membrane were measured five times for each frequency and averaged using a custom-made program. Subsequently, the miniaturized device was manually inserted into the scala tympani with its piezoelectric membrane adjacent to the basilar membrane. The laser beam was directed to a glass bead either placed on the surface of the piezoelectric membrane (Fig. 3) or fixed on the silicon frame (Fig. 3) of the implantable device for reflection to detect vibrations.

Miniaturized Device for Voltage Output Recording. The design of an implantable miniaturized device for vibration measurement was modified to record the voltage output from the piezoelectric membrane after implan-

tation into a cochlea. An implantable miniaturized device was connected to a silicon rod carrying electrodes for monitoring the voltage output from the piezoelectric membrane. Two thin (40-nm thickness) gold electrodes, which faced the basilar membrane of the cochlea, were formed by thermal deposition on the piezoelectric membrane. One thin (100-nm thickness) platinum electrode was formed by rf magnetron sputtering on the opposite side of the piezoelectric membrane for recording the output voltage.

Recording Voltage Output from the Piezoelectric Membrane in Response to Sound Stimuli. Two right temporal bones of guinea pigs were used. The bony wall of the otic bulla was removed to expose the basal portion of the cochleae and the incudostapedial joint. After separating the head of the stapes from the incus, the tympanic membrane, malleus, and incus were removed. Cochleostomy of the basal portion of cochleae was performed to access the scala tympani. The temporal bones were then fixed on a stage. The head of the stapes and an actuator (AE0203D04F; NEC/TOKIN) were connected with a needle. The position of the tip of the needle was monitored by a CCD camera during the recording. Tone-burst signals were delivered to an actuator using a function generator (NF Corporation). A modified miniaturized device was inserted into the scala tympani of the basal portion of the cochleae through the cochleostomy site, and it was attached to the piezoelectric membrane and the basilar membrane using a micromanipulator. The scala tympani was filled with 285 mM mannitol solution during the recording. The voltage outputs from the piezoelectric membrane were transmitted to a custom-made amplifier that produced a 1,000-fold increase, and their waveforms and amplitudes were monitored with an oscilloscope (WaveRunner 44MXi-A; LeCroy).

ACKNOWLEDGMENTS. The authors thank Shin-ichiro Kitajiri and Norio Yamamoto for technical contributions to histological analyses and Kozo Kumakawa, Yasushi Naito, and Harukazu Hiraumi for contributions to the development of surgical procedures. This study was supported by grants for Research on Sensory and Communicative Disorders from the Japanese Ministry of Health, Labor and Welfare (to J.I.).

1. Dallos P (1996) *The Cochlea*, eds Dallos P, Popper AN, Fay RR (Springer, New York), pp 1–43.
2. Sarpeshkar R, Lyon RF, Mead C (1998) A low-power wide-dynamic-range analog VLSI cochlea. *Analog Integr Circuits Signal Process* 16:245–274.
3. Slepecky NB (1996) *The Cochlea*, eds Dallos P, Popper AN, Fay RR (Springer, New York), pp 44–129.
4. von Békésy G (1960) *Experiments in Hearing*, ed Wever EG (McGraw-Hill, New York), pp 404–429.
5. von Békésy G (1970) Travelling waves as frequency analysers in the cochlea. *Nature* 225:1207–1209.
6. Patuzzi R (1996) *The Cochlea*, eds Dallos P, Popper AN, Fay RR (Springer, New York), pp 186–257.
7. Belyantseva IA, Adler HJ, Curi R, Frolenkov GI, Kachar B (2000) Expression and localization of prestin and the sugar transporter GLUT-5 during development of electromotility in cochlear outer hair cells. *J Neurosci* 20:RC116.
8. Davis H (1983) An active process in cochlear mechanics. *Hear Res* 9:79–90.
9. Evans BN, Dallos P (1993) Stereocilia displacement induced somatic motility of cochlear outer hair cells. *Proc Natl Acad Sci USA* 90:8347–8351.
10. Zheng J, et al. (2000) Prestin is the motor protein of cochlear outer hair cells. *Nature* 405:149–155.
11. Liberman MC, et al. (2002) Prestin is required for electromotility of the outer hair cell and for the cochlear amplifier. *Nature* 419:300–304.
12. LeMasurier M, Gillespie PG (2005) Hair-cell mechanotransduction and cochlear amplification. *Neuron* 48:403–415.
13. Liberman MC, Rosowski JJ, Lewis RF (2010) *Schuknecht's Pathology of the Ear*, eds Merchant SN, Nadol JB (People's Medical Publishing House-USA, Shelton, CT), 3rd Ed, pp 104–127.
14. Merchant SN (2010) *Schuknecht's Pathology of the Ear*, eds Merchant SN, Nadol JB (People's Medical Publishing House-USA, Shelton, CT), 3rd Ed, pp 631–663.
15. Diaz RC (2009) Inner ear protection and regeneration: A 'historical' perspective. *Curr Opin Otolaryngol Head Neck Surg* 17:363–372.
16. Oshima K, Suchert S, Blevins NH, Heller S (2010) Curing hearing loss: Patient expectations, health care practitioners, and basic science. *J Commun Disord* 43:311–318.
17. Zeng FG, Rebscher S, Harrison WV, Sun X, Feng H (2008) Cochlear implants: System design, integration and evaluation. *IEEE Rev Biomed Eng* 1:115–142.
18. Shintaku H, et al. (2010) Development of piezoelectric acoustic sensor with frequency selectivity for artificial cochlea. *Sens Actuators A* 158:183–192.
19. Yamane H, Marsh RR, Potsic WP (1981) Brain stem response evoked by electrical stimulation of the round window of the guinea pig. *Otolaryngol Head Neck Surg* 89: 117–124.
20. Viberg A, Canlon B (2004) The guide to plotting a cochleogram. *Hear Res* 197:1–10.
21. Wada H, Homma Y, Takahashi S, Takasaka T, Ohyama K (1996) *Proceedings of the International Symposium on Diversity in Auditory Mechanics*, eds Lewis ER, et al. (World Scientific, Teaneck, NJ), pp 284–290.
22. Helle R (1977) Investigation of the vibrational processes in the inner ear with the aid of hydromechanical models. *J Audiol Techn* 16:138–163.
23. Chadwick RS, Fourney ME, Neiswander P (1980) Modes and waves in a cochlear model. *Hear Res* 2:475–483.
24. Lechner TP (1993) A hydromechanical model of the cochlea with nonlinear feedback using PVF2 bending transducers. *Hear Res* 66:202–212.
25. Zhou G, Bintz L, Anderson DZ, Bright KE (1993) A life-sized physical model of the human cochlea with optical holographic readout. *J Acoust Soc Am* 93:1516–1523.
26. Chen F, et al. (2006) A hydromechanical biomimetic cochlea: Experiments and models. *J Acoust Soc Am* 119:394–405.
27. Wittbrodt MJ, Steele CR, Puria S (2006) Developing a physical model of the human cochlea using micro-fabrication methods. *Audiol Neurootol* 11:104–112.
28. White RD, Grosh K (2005) Microengineered hydromechanical cochlear model. *Proc Natl Acad Sci USA* 102:1296–1301.
29. Bachman M, Zeng FG, Xu T, Li GP (2006) Micromechanical resonator array for an implantable bionic ear. *Audiol Neurootol* 11:95–103.
30. Ogita H, et al. (2009) Surgical invasiveness of cell transplantation into the guinea pig cochlear modiolus. *ORL J Otorhinolaryngol Relat Spec* 71:32–39.
31. Shintaku H, et al. (2010) Culturing neurons on MEMS fabricated P(VDF-TrFE) films for implantable artificial cochlea. *J Biomech Sci Eng* 5:229–235.
32. Nilsen KE, Russell IJ (1999) Timing of cochlear feedback: Spatial and temporal representation of a tone across the basilar membrane. *Nat Neurosci* 2:642–648.
33. Wada H, et al. (1999) Measurement of dynamic frequency characteristics of guinea pig middle ear by a laser Doppler velocimeter. *JSME Int J Ser C* 42:753–758.

Mutai et al. BMC Medical Genetics 2011, 12:135
http://www.biomedcentral.com/1471-2350/12/135

BMC Medical Genetics

RESEARCH ARTICLE Open Access

Systematic analysis of mitochondrial genes associated with hearing loss in the Japanese population: dHPLC reveals a new candidate mutation

Hideki Mutai[1], Hiroko Kouike[1], Eiko Teruya[1], Ikuko Takahashi-Kodomari[1], Hiroki Kakishima[2], Hidenobu Taiji[3], Shin-ichi Usami[4], Torayuki Okuyama[2] and Tatsuo Matsunaga[1*]

Abstract

Background: Variants of mitochondrial DNA (mtDNA) have been evaluated for their association with hearing loss. Although ethnic background affects the spectrum of mtDNA variants, systematic mutational analysis of mtDNA in Japanese patients with hearing loss has not been reported.

Methods: Using denaturing high-performance liquid chromatography combined with direct sequencing and cloning-sequencing, Japanese patients with prelingual (N = 54) or postlingual (N = 80) sensorineural hearing loss not having pathogenic mutations of m.1555A > G and m.3243A > G nor *GJB2* were subjected to mutational analysis of mtDNA genes (*12S rRNA*, $tRNA^{Leu(UUR)}$, $tRNA^{Ser(UCN)}$, $tRNA^{Lys}$, $tRNA^{His}$, $tRNA^{Ser(AGY)}$, and $tRNA^{Glu}$).

Results: We discovered 15 variants in *12S rRNA* and one homoplasmic m.7501A > G variant in $tRNA^{Ser(UCN)}$; no variants were detected in the other genes. Two criteria, namely the low frequency in the controls and the high conservation among animals, selected the m.904C > T and the m.1105T > C variants in *12S rRNA* as candidate pathogenic mutations. Alterations in the secondary structures of the two variant transcripts as well as that of m.7501A > G in $tRNA^{Ser(UCN)}$ were predicted.

Conclusions: The m.904C > T variant was found to be a new candidate mutation associated with hearing loss. The m.1105T > C variant is unlikely to be pathogenic. The pathogenicity of the homoplasmic m.7501T > A variant awaits further study.

Background

Hearing loss manifests in more than 1 in 1000 persons at birth, and the frequency increases subsequently to 3 in 1000 by 4 years of age [1,2]. Approximately 50 to 70% of congenital and childhood deafness is estimated to be due to genetic mutations. In adults, the prevalence of hereditary hearing impairment has been estimated to be approximately 3.2 in 1000 [3]. Some of the mitochondrial DNA (mtDNA) genes, such as *12S rRNA*, $tRNA^{Leu(UUR)}$, and $tRNA^{Ser(UCN)}$, are known to be responsible for hereditary hearing loss [4]. Among them, the m.1555A > G mutation in *12S rRNA* is found relatively frequently (0.6-16%, depending on the ethnic group) in aminoglycoside-induced, congenital, and late-onset nonsyndromic hearing loss [4,5]. The m.1494C > T mutation in *12S rRNA* is also associated with aminoglycoside-induced and nonsyndromic hearing loss [6,7]. The m.3243A > G mutation in $tRNA^{Leu(UUR)}$ is associated with late-onset nonsyndromic hearing loss [8,9], maternally inherited diabetes and deafness (MIDD) [10,11], and mitochondrial myopathy, encephalopathy, lactic acidosis, stroke-like episodes (MELAS), which frequently presents with hearing loss [12,13]. The m.7445A > C/G/T [14-16], 7472insC [17], and 7510T > C mutations [18] in $tRNA^{Ser(UCN)}$ are also associated with

* Correspondence: matsunagatatsuo@kankakuki.go.jp
[1]Laboratory of Auditory Disorders, Division of Hearing and Balance Research, National Institute of Sensory Organs, National Tokyo Medical Center, Tokyo, Japan
Full list of author information is available at the end of the article

aminoglycoside-induced, nonsyndromic, or syndromic hearing loss.

In addition, many other variants in *12S rRNA* have been proposed to be associated with hearing loss [4]. Some variants such as m.827A > G [19,20], 961T > C [21], 961delT + Cn [21,22], 1005T > C [22], and 1095T > C in *12S rRNA* [22-26] are not definitively related to hearing loss, because they have been found in subjects with normal hearing and/or are not conserved among mammals [19,27-30]. Moreover, a variety of mitochondrial haplogroups often localize in specific ethnic groups, making it difficult to determine whether the mtDNA variants are associated directly with diseases, indirectly as risk factors, or simply with rare subhaplogroups [31-34]. Accumulating reports of various novel mtDNA mutations associated with hearing loss prompted us to evaluate these variants in patients with hearing loss in Japan, where mtDNA mutation studies have focused on a few limited nucleotide positions [35,36].

A single cell contains hundreds of mitochondria, and the mtDNA in each mitochondrion is occasionally heterogeneous, a feature called heteroplasmy [37]. The proportion of pathogenic mutations of heteroplasmic mtDNA is considered to be one of the reasons for the wide range of severity of phenotypes seen in patients with mitochondrial-related diseases, such as those reported in the case of the m.3243A > G mutation [38-40]. Denaturing high-performance liquid chromatography (dHPLC) is a sensitive method to detect heteroplasmic mutations that can be overlooked by simple direct sequencing and comparison of the scanned peaks or restriction fragment length polymorphism-PCR [28,41]. In this study, we conducted a systematic mutational analysis of mtDNA by dHPLC combined with direct sequencing and cloning-sequencing in samples from Japanese patients with hearing loss.

Methods

Subjects

Subjects with bilateral sensorineural hearing loss were recruited by the National Tokyo Medical Center and collaborating hospitals. Subjects' medical histories were obtained and physical examinations were performed to exclude those subjects with syndromic symptoms, diseases of the outer or/and middle ear, and environmental factors related to hearing loss such as history of infectious diseases, premature birth, and newborn meningitis. Patients with a history of use of ototoxic drugs were included in the study because these drugs are known to be associated with mitochondrial hearing loss. Prior to this study, the patients were confirmed not to have the m.1555A > G and m.3243A > G mutations or not to be diagnosed as having *GJB2* -caused hearing loss, as assessed by restriction fragment length polymorphism-PCR or together with direct sequencing if the heterozygotic 235delC mutation was detected in *GJB2* [42,43]. The 134 subjects were classified into prelingual hearing loss (onset before 5 years old, 20 males and 34 females) or postlingual hearing loss (onset at 5 years old or later, 31 males and 49 females) [1]. The control group consisted of 137 unrelated Japanese individuals with normal hearing as examined by pure-tone audiometry. All subjects or their parents gave prior informed consent for participation in this study. This study was approved by the ethics committee of National Tokyo Medical Center.

Screening for mtDNA mutations by dHPLC

DNA was extracted from blood samples using the Gentra Puregene DNA isolation kit (QIAGEN, Hamburg, Germany). Initially, whole mtDNA from each patient was amplified in three overlapping fragments (1351-8197, 6058-12770, and 11706-2258) [44] by LATaq DNA polymerase (TaKaRa BIO, Shiga, Japan). PCR was conducted at 94°C for 1 min followed by 30 cycles of 98°C for 10 s and 68°C for 6.5 min. Then, using the PCR products as templates, variants were analyzed by the Mitoscreen assay kit (Transgenomic, Glasgow, UK). We amplified the genes *12S rRNA*, $tRNA^{Leu(UUR)}$, $tRNA^{Ser(UCN)}$, $tRNA^{Lys}$, $tRNA^{His}$, $tRNA^{Ser(AGY)}$, and $tRNA^{Glu}$, for which mutations were reported to be associated with hearing loss on the Hereditary Hearing Loss Homepage [45] when the study was started. The PCR products using primer sets MT4 (for *12S rRNA*), MT6 ($tRNA^{Leu(UUR)}$), MT10 ($tRNA^{Ser(UCN)}$), MT11 ($tRNA^{Lys}$), MT15 ($tRNA^{His}$ and $tRNA^{Ser(AGY)}$), and MT18 ($tRNA^{Glu}$) were incubated with the appropriate restriction enzymes, incubated for heteroduplex formation either with reference PCR products to detect homoplasmy or with their own PCR products to detect heteroplasmy, then analyzed by dHPLC (WAVE system, Transgenomic) according to the manufacturer's protocols.

The reference mtDNA was derived from a Japanese individual with normal hearing. Sequencing of the entire reference mtDNA revealed 750A > G and 1438A > G polymorphisms, and the mtDNA sequence was otherwise comparable to the revised Cambridge Reference sequence (AC_000021) [46,47]).

DNA sequencing

When homoplasmic or heteroplasmic variants were detected, the PCR product was subjected to direct sequencing by the BigDye Terminator ver. 3 cycle sequencing kit and ABI genetic analyzer 3730 (Life Technologies, Carlsbad, CA). To sequence *12S rRNA*, an additional nested PCR product (656-1,266) was amplified with primers F (5'-tggtcctagcctttctattagctctt-3') and R (5'-tggcggtataggctgagca-3'). To sequence $tRNA^{Ser}$

$^{(UCN)}$, an additional nested PCR product (7,209-7,609) was amplified with primers F (5'-atgccccgacgttactcg-3') and R (5'- acctacttgcgctgcatgtg-3'). To determine the proportion of heteroplasmic 1005T > C variant in the *12S rRNA*, the nested PCR (656-1,266) product was cloned and sequenced. Nested PCR was carried out by replacing AmpliTaq Gold DNA polymerase with PrimeSTAR DNA polymerase, which has 3'-proofreading activity (TaKaRa BIO), followed by the Zero Blunt TOPO PCR cloning kit (Life Technologies). We sequenced 54 clones derived from the proband mtDNA and 24 clones derived from the mtDNA of each of five siblings. Sequencing data were analyzed by SeqScape ver2.6 (Life Technologies) and DNASIS Pro (Hitachisoft, Tokyo, Japan). The sequencing results for each patient were compared with the revised Cambridge Reference sequence to identify mtDNA variants. The uniqueness of each mutation was evaluated by comparison with the mtSNP database [48], MITOMAP [49], and the Uppsala mtDB database [50].

Prediction of pathogenicity of mtDNA variants

The variants were evaluated based on double selection as proposed by Leveque and coworkers [51], with modification. Initially, we measured the frequencies of each variant found in the controls in our study (N = 137) and in the mtSNP database (N = 672, including: centenarians in Gifu, centenarians in Tokyo, type 2 diabetes mellitus patients (without or with vascular disorders), overweight young adult males, non-overweight young adult males, Parkinson's disease patients, and Alzheimer's disease patients in Japan). The variants with a frequency of more than 3% in one of the groups were considered as non-pathologic polymorphisms. We used a frequency threshold lower than that previously used (4%) [51] because the mtSNP database of Japanese individuals and the controls reflect the patient ethnic group background more closely than the mtDB and therefore requires a lower frequency threshold to exclude polymorphisms. The nucleotide conservation in each gene from human and 50 mammalian species was evaluated by ClustalW. The additional file lists the mammalian species and the accession numbers of the mtDNA (Additional File 1: Table S1). The variant frequencies in the mtDB were calculated to determine if the low variant frequencies measured in the controls reflect rare haplotypes in the Japanese population and are more common worldwide. All the variants were also analyzed with PhyloTree (mtDNA tree Build 10) [52] to search for previously characterized variants in haplogroups. Pathogenicity of the variants was also evaluated by predicting the secondary structures of the mitochondrial transcripts with or without the variant using Centroid Fold [53,54].

Results

dHPLC screening and subsequent direct sequencing in the patients identified 12 homoplasmic or heteroplasmic variants in *12S rRNA* and 1 homoplasmic variant in $tRNA^{Ser(UCN)}$ (Table 1). In addition, the 3 homoplasmic variants, m.752C > T, 1009C > T, and 1107T > C in *12S rRNA* were detected in the controls by direct sequencing. All the patients and the controls appeared to have the non-pathogenic m.750A > G and 1438A > G variants, as previously noted [49]. No $tRNA^{Glu}$, $tRNA^{Leu\ (UUR)}$, $tRNA^{Lys}$, $tRNA^{His}$, or $tRNA^{Ser(AGY)}$ variants were detected. Table 1 lists the number of patients found with each variant, the frequencies of the variants in the controls and among Japanese individuals with various clinical conditions (mtSNP, N = 672), previous reports of the variants, and the frequencies of the variants in the mtDB. We evaluated two criteria, namely that the frequency of the variants be < 3% in both the controls and in the Japanese database (mtSNP) and that the variant nucleotide conserved by >50% among the 51 mammalian species we considered [51]; based on this analysis, two *12S rRNA* variants, m.904C > T and 1005T > C, were selected as candidate pathogenic mutations and subjected to further study. Although the homoplasmic m.7501T > A variant in $tRNA^{Ser(UCN)}$ did not meet the conservation criteria, it was also subjected to further study because several other $tRNA^{Ser(UCN)}$ mutations have been reported to be associated with hearing loss, whereas the m.7501T > A variant has not been studied for its pathogenicity.

A novel homoplasmic m.904C > T variant in the*12S rRNA* was found in a 46-year-old female patient (Figure 1A). She did not possess additional mtDNA pathogenic mutations and showed prelingual, progressive hearing loss with tinnitus. The patient was suspected of hearing impairment as early as 4 years old and was diagnosed with sensorineural hearing loss at age 11. The audiometric examination showed mild hearing loss at low frequencies and no response at 1 kHz and higher frequencies (Figure 1B). She had no response to an otoacoustic emission test, indicating dysfunction of the auditory outer hair cells. The patient had no history of treatment with ototoxic drugs and did not suffer from any other symptoms. The siblings also suffered from prelingual, severe hearing loss (with similar ages of onset and severity), but their parents had normal hearing (Figure 1A). The patient bore two children with normal hearing. DNA samples were not obtained from other family members. The secondary structure of the variant 12S rRNA predicted by Centroid Fold suggested that substitution of C > T (transcribed as U) at position 904 of the *12S rRNA* results in gross structural alteration of the transcript region that includes nucleotide positions 862 to 917, in addition to truncation of the